Indian Journal of Biochemistry & Biophysics
Vol. 63, October 2026, pp. 1213-1231
DOI: 10.56042/ijbb.v63i10.21526

Oldenlandia umbellata as a promising agent for obesity management: Enzyme inhibition and antiadipogenic effects

Athista Manoharan[1], Prakash Pandurangan[2], Jayshree Nellore[2], Valli Nachiyar Chandrasekaran[3] & Swetha Sunkar[1]*

[1]Department of Bioinformatics; & [2]Department of Biotechnology, Sathyabama Institute of Science and Technology, Chennai-600 119, Tamil Nadu, India

[3]Department of Research, Meenakshi Academy of Higher Education and Research, Chennai-600 087, Tamil Nadu, India

Received 11 July 2025; *revised 15 August 2026*

Obesity is a major global health challenge associated with metabolic disorders and the need for effective interventions, particularly from natural sources. This study evaluated the metabolic enzyme inhibitory and anti-adipogenic potential of *Diospyros ebenum* and *Oldenlandia umbellata* ethanolic extracts using *in vitro* assays and a 3T3-L1 preadipocyte model. Both extracts exhibited inhibitory activity against α-amylase, α-glucosidase, and pancreatic lipase, with *O. umbellata* showing comparatively stronger inhibition particularly against α-glucosidase, and pancreatic lipase. Cytotoxicity assessment indicated no substantial cytotoxicity of the extracts toward Vero cells at concentrations ≤100 µg/mL under the tested conditions. Treatment of 3T3-L1 adipocytes with *O. umbellata* extract significantly reduced intracellular lipid accumulation and triglyceride levels. Gene-expression analysis showed reduced PPARγ and FAS expression and increased adiponectin expression compared with differentiated controls, whereas SREBP-1c was not significantly altered and leptin showed modest increase. *In silico* ADME and toxicity analyses indicated favorable predicted pharmacokinetic and drug-likeness characteristics for several putatively identified phytoconstituents. Overall, the findings support the potential of *O. umbellata* as a source of bioactive compounds with enzyme inhibitory and anti-adipogenic activities. Further studies are required to identify the active constituents, elucidate the underlying molecular mechanisms, and validate these effects in appropriate *in vivo* models.

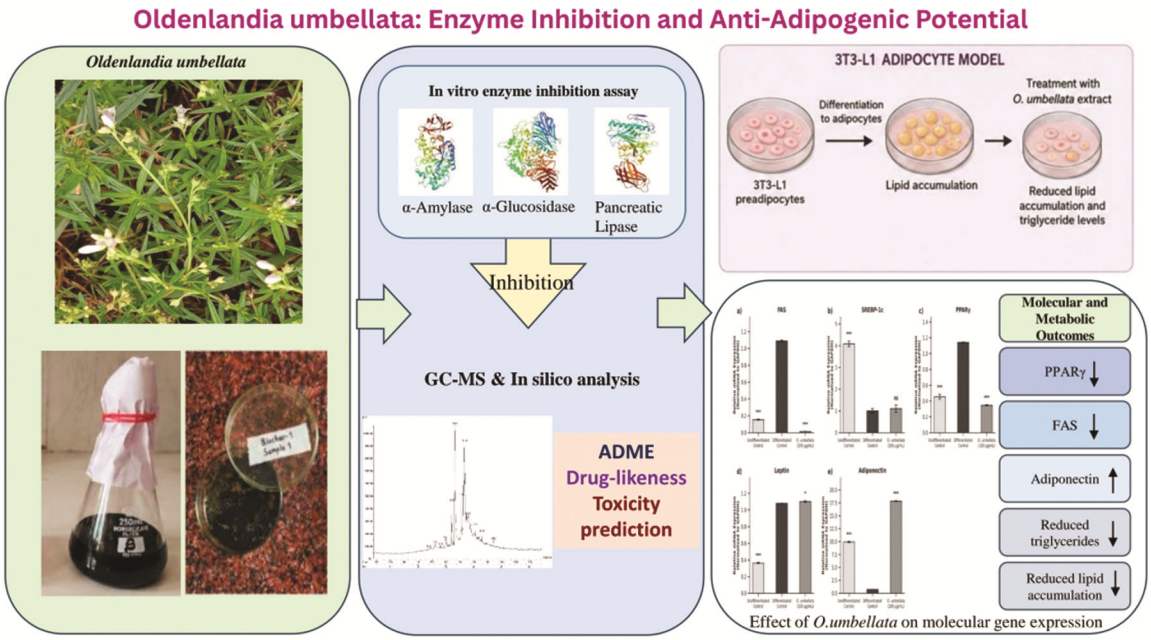
Keywords: 3T3-L1 Preadipocytes, Adipogenesis, *Diospyros ebenum*, Enzymes, *Oldenlandia umbellata*

Obesity is a multifactorial metabolic disorder characterized by excessive accumulation of adipose tissue and represents a significant global health concern. According to the World Health Organization, obesity prevalence has nearly tripled worldwide over the past decades, contributing to increased incidences of cardiovascular diseases, type 2 diabetes, and certain cancers, thereby reducing life expectancy and affecting psychosocial well-being[1]. While genetic, physiological, and environmental factors contribute to obesity, sedentary lifestyles coupled with high-calorie diets remain major contributing factors in many populations.

Adipose tissue plays a critical role in maintaining energy homeostasis, and its expansion during obesity is primarily due to hypertrophy and hyperplasia of adipocytes[2]. Adipogenesis, the process through which preadipocytes differentiate into mature adipocytes, is tightly regulated by transcription factors, including peroxisome proliferator-activated receptor gamma (PPARγ), CCAAT/enhancer-binding protein alpha (C/EBPα), and sterol regulatory element-binding protein 1c (SREBP-1c)[3]. These transcription factors regulate the expression of adipogenic and lipogenic genes, including fatty acid synthase (FAS), thereby promoting lipid accumulation in adipocytes[4]. Consequently, modulation of adipocyte differentiation and lipid accumulation represents an important experimental strategy for investigating potential interventions relevant to obesity.

Pharmacological interventions for obesity often focus on inhibiting digestive enzymes, such as α-amylase, α-glucosidase, and pancreatic lipase, which play critical roles in carbohydrate and fat digestion. α-amylase and α-glucosidase inhibitors decrease carbohydrate breakdown, while pancreatic lipase inhibitors such as orlistat reduce fat absorption, thereby helping to control postprandial glucose excursions and energy intake[5-8]. However, the long-term use of synthetic inhibitors may be associated

*Correspondence:
E-mail: swethauk78@gmail.com
Suppl. data available on respective page of NOPR



Graphical abstract

with adverse effects, including gastrointestinal discomfort and other tolerability concerns, thereby encouraging the exploration of alternative sources of bioactive compounds.

Natural products, particularly plant-based compounds, have gained attention as potential sources of bioactive molecules, including flavonoids, polyphenols, and alkaloids, which have been associated with antioxidant, anti-inflammatory, and metabolic regulatory activities[9]. Several medicinal plants have shown potential in modulating lipid metabolism and inhibiting adipogenesis, presenting opportunities for the development of plant-derived interventions relevant to obesity. However, many plants with traditional medicinal use remain insufficiently investigated for their effects on adipocyte differentiation and metabolic enzyme activity.

Diospyros ebenum (*D. ebenum*) and *Oldenlandia umbellata* (*O. umbellata*) are two such plants with a history of use in traditional medicine for various ailments, including inflammation, infections, and hepatoprotection[10-12]. *Diospyros* species are known for their rich phytochemical content, including flavonoids and polyphenols with antioxidant potential, while *O. umbellata* has been reported to exhibit antibacterial, antioxidant, anti-inflammatory, antipyretic, immunomodulatory, hepatoprotective, antitussive, and antitumor activities, indicating its broad pharmacological potential[13-16]. Despite these reported bioactivities, the potential role of *O. umbellata* in obesity-related metabolic processes has not been adequately investigated. To the best of our knowledge, the effects of *O. umbellata on* pancreatic lipase inhibition and 3T3-L1 adipocyte differentiation have not been previously reported. In addition, its effects on intracellular lipid accumulation, triglyceride content, and the expression of key adipogenic and lipogenic genes, including PPARγ, SREBP-1c, FAS, adiponectin, and leptin, have not been clearly studied.

Although related species within the *Diospyros* and *Oldenlandia* genera have demonstrated metabolic and pharmacological activities, evidence specifically linking *O. umbellata* to adipocyte differentiation, lipid accumulation, and the regulation of adipogenic gene expression remains limited. An integrated evaluation combining metabolic enzyme inhibition with cellular and molecular assessment of adipogenesis may therefore provide a more comprehensive understanding of the biological potential of this plant.

In this study, we aimed to evaluate the metabolic enzyme inhibitory and anti-adipogenic potential of ethanolic extracts of *D. ebenum* and *O. umbellata through in vitro* enzyme inhibition assays targeting α-amylase, α-glucosidase, and pancreatic lipase, together with adipogenesis studies using the 3T3-L1 preadipocyte model. The present study extends previous investigations of *O. umbellata*, which have primarily focused on its enzyme inhibitory and other

pharmacological activities, by evaluating its effects at the cellular level. The study further assessed intracellular lipid accumulation, triglyceride content, and the expression of selected adipogenic and lipogenic genes, including PPARγ, SREBP-1c, FAS, adiponectin, and leptin. In addition, the evaluation of pancreatic lipase inhibition extends the investigation beyond the enzyme activities previously reported for *O. umbellata*. Together, these analyses provide an integrated *in vitro* assessment of the enzymatic, cellular, biochemical, and molecular effects of *O. umbellata*.

Materials and Methods

Plant collection and authentication

A powdered sample of *D. ebenum* bark was obtained from a local herbal supplier, while fresh whole plants of *O. umbellata* were collected from their natural habitat in Nagercoil, Tamil Nadu, India. The collected *O. umbellata* plant material was authenticated. The plant materials were shade-dried, powdered separately, and stored in airtight containers until extraction and further analysis.

Preparation of plant extracts

The powdered plant samples (50 g) were extracted separately with 200 mL of each solvent, namely petroleum ether, ethyl acetate, ethanol, and water. For each solvent extraction, a separate 50 g portion of the powdered plant material was used; the solvents were not applied sequentially to the same plant material. A plant material-to-solvent ratio of 1:4 (*w/v*) was maintained for each extraction. Cold maceration was carried out for 72 h with intermittent shaking. Each extract was filtered through Whatman No. 1 filter paper, and the filtrate was concentrated by removing the solvent using a rotary evaporator under reduced pressure. The concentrated extracts were stored at 4°C until further analysis[17].

Preliminary phytochemical analysis

The preliminary phytochemical screening of the extracts was carried out using standard qualitative biochemical assays to find the major classes of phytoconstituents present such as alkaloids, carbohydrates, proteins, steroids, flavonoids, triterpenoids, phenols, tannins and saponins[18]. This result was used for comparing phytochemical profiles among plant extracts from various solvents and was utilized for subsequent biological evaluation.

Test for alkaloids: About 1 mL of the plant extract was treated with about 2 mL of Mayer's reagent. The formation of a precipitate indicated the presence of alkaloids.

Test for Carbohydrates: About 3 mL of plant extract was mixed with 2 mL of Molisch's reagent and shaken well and then add about 2 mL of conc. sulphuric acid down through the side of the test-tube. Red color or muddy-violet color at interface indicated presence of carbohydrate.

Test for Flavonoids: The plant extract was treated with few drop of sodium hydroxide which turns colorless upon the addition of dilute acid.

Test for Phenols: About 2 mL of the plant extract was mixed with 2 mL of distilled water. Then few drop of 10 % solution of ferric chloride ($Fecl_3$) are added. The development of a bluish-black color is suggestive for the presence of phenol.

Test for proteins: About 2 mL of the plant extract was heated and cooled to room temperature. A few drops of 40% sodium hydroxide (NaOH) solution and 1% copper sulfate ($CuSO_4$) solution were then added, and the mixture was shaken well. The development of a violet colour indicated the presence of proteins.

Test for saponins: A small quantity of water and two drops of coconut oil were added to the extract. The formation of persistent foam or a layer indicated the presence of saponins.

Test for steroids: About 2 mL of the plant extract was treated with 2 mL of acetic acid and heated. After cooling, concentrated sulfuric acid was added. The formation of a green-coloured upper layer indicated the presence of steroids.

Test for tannins: To about 5 mL of the plant extract, 2 mL of 5% ferric chloride solution was added and after few min greenish black color or precipitate obtained.

Test for triterpenoids: About 2 mL of chloroform was mixed with the plant extract and evaporated on a water bath. The residue was then treated with 2 mL of concentrated sulfuric acid. The development of a grey colour indicated the presence of triterpenoids.

Cell lines and reagents

Porcine pancreatic α-amylase, porcine pancreatic lipase, and Saccharomyces cerevisiae α-glucosidase were procured from Sigma-Aldrich. 3T3-L1 preadipocytes and Vero cell lines were obtained from the National Centre for Cell Science (NCCS), Pune, India. All other reagents used were of analytical grade.

Cytotoxicity assay on Vero cells

The MTT assay was performed to evaluate the cytotoxicity of the plant extracts toward Vero cells[19].

Cells were seeded at 1 × 10^4 cells/well in 96-well plates and incubated at 37°C in a humidified atmosphere containing 5% CO_2 for 24 h. Cells were treated with the extracts at concentrations ranging from 100 to 500 µg/ mL for 24 h, followed by the addition of 20 µL of MTT solution (5 mg/ mL) and incubation for 4 h. The resulting formazan crystals were dissolved in 100 µL of DMSO, and absorbance was measured at 540 nm using a microplate reader. Cell viability was expressed as a percentage relative to the untreated control group.

The percentage of cell growth inhibition was calculated using the following formula:

Percentage inhibition of cell proliferation = [(Mean absorbance of control − Mean absorbance of treated sample) / Mean absorbance of control] × 100

In vitro enzyme inhibition assays

α-amylase inhibition assay

The α-amylase inhibitory activity of the plant extracts was evaluated using a modified method adapted from McCue and Shetty, 2004[20]. Various concentrations of the extract (20, 40, 60, 80, and 100 µg/ mL) were prepared, and 250 µL of each concentration was transferred into separate test tubes. To each tube, 250 µL of α-amylase enzyme solution (0.5 mg/ mL) prepared in 0.02 M sodium phosphate buffer (pH 6.9) was added. The mixtures were pre-incubated at 25°C for 10 min. Following the pre-incubation, 250 µL of 1% starch solution (also prepared in 0.02 M sodium phosphate buffer, pH 6.9) was added at fixed intervals to initiate the reaction. The reaction mixtures were incubated again at 25°C for another 10 min. To terminate the enzymatic reaction, 500 µL of dinitrosalicylic acid (DNSA) reagent was added to each tube. The tubes were then heated in boiling water for 5 min and subsequently allowed to cool to room temperature. After cooling, 5 mL of distilled water was added to each tube, and the absorbance was measured at 540 nm using a UV-visible spectrophotometer. Acarbose was used as the reference standard for comparison.

The percentage of α-amylase inhibition was calculated using the following formula:

Inhibition (%) = ((Absorbance of control – Absorbance of sample) /Absorbance control) ×100

α-glucosidase inhibition assay

The α-glucosidase inhibitory activity of the plant extracts was assessed following a modified procedure[21]. The enzyme solution was prepared by dissolving yeast α-glucosidase (0.7 U) in 100 mM phosphate buffer (pH 7.0) containing 2 g/L bovine serum albumin and 0.2 g/L sodium azide. The substrate solution consisted of 5 mM p-nitrophenyl-α-D-glucopyranoside prepared in the same buffer. For the assay, 1000 µL of the enzyme solution was mixed with 100 µL of the plant extract at different concentrations (20, 40, 60, 80, and 100 µg/ mL). The mixture was incubated for 5 min at room temperature. Following the incubation, 50 µL of the substrate solution was added to initiate the reaction, and the mixture was incubated again for 5 min. After the reaction period, the change in absorbance was measured at 405 nm using a UV-Vis spectrophotometer (Model: UV1800, Shimadzu, Japan). Acarbose was used as the standard inhibitor.

Pancreatic lipase inhibition assay

The inhibitory effect of the ethanolic plant extracts on pancreatic lipase activity was evaluated using a modified spectrophotometric method[22]. A substrate emulsion was prepared by mixing 1% (*v/v*) triolein and 1% (*v/v*) Tween 40 in 0.1 M phosphate buffer (pH 8.0), followed by thorough emulsification. To initiate the assay, 1600 µL of the triolein emulsion was combined with 200 µL of porcine pancreatic lipase solution, which was prepared by dissolving 0.5 g of pancreatin in 15 mL of 0.1 M phosphate buffer (pH 8.0). Additionally, 200 µL of plant extract at varying concentrations (25, 50, 100, 200, and 400 µg/ mL) was added to the reaction mixture. Immediately after mixing, the absorbance was measured at 450 nm to establish a baseline. The reaction mixtures were then incubated at 37°C for 30 min, after which the absorbance was recorded again at 450 nm. Orlistat was used as a positive control for comparison. For all enzyme inhibition assays, an enzyme control without plant extract was used to represent 100% enzyme activity, and appropriate sample blanks without enzyme were included to account for background absorbance from the plant extracts and assay reagents. Each enzyme inhibition assay was independently performed three times (n=3 independent experiments), and the results were expressed as mean ± SD.

GC-MS analysis and *in silico* pharmacokinetics

The ethanolic extract of *O. umbellata* was subjected to phytochemical profiling using a Shimadzu GC–MS QP2020 system equipped with a fused silica capillary column (30 m × 0.25 mm

internal diameter × 0.25 µm film thickness). Helium was used as the carrier gas at a flow rate of 1.0 mL/min. The injection volume was 1 µL, and the injector temperature was maintained at 250 °C. The oven temperature was initially set at 60 °C and held for 2 min, followed by an increase at a rate of 10 °C/min to 280 °C, which was maintained for 10 min. Mass spectrometric detection was performed using electron ionization (EI) at an ionization energy of 70 eV. The compounds were analyzed in full-scan mode over an *m/z* range of 50–650. The detected compounds were identified by comparing their mass spectra and relative retention times with reference data available in the National Institute of Standards and Technology (NIST) and Wiley spectral libraries and with published literature data. As authentic reference standards were not used for confirmation, the identified compounds were considered putatively identified. The relative abundance of the detected compounds was estimated based on their corresponding peak areas[23]. The putatively identified phytoconstituents of the ethanolic extract of *O. umbellata* were subjected to *in silico* ADME, drug-likeness, and toxicity prediction. SwissADME was used to evaluate physicochemical and pharmacokinetic properties, including molecular weight, lipophilicity (iLogP), topological polar surface area (TPSA), hydrogen-bond donors and acceptors, gastrointestinal absorption, and drug-likeness based on Lipinski's rule of five. OSIRIS Property Explorer was used to assess cLogP, aqueous solubility, drug-likeness, drug score, and structural toxicity alerts, including mutagenic, tumorigenic, irritant, and reproductive toxicity risks. ProTox-3.0 was used to predict acute oral toxicity (LD_{50} and toxicity class) and selected toxicity endpoints based on the available prediction models. The compounds were prioritized based on their overall ADME, drug-likeness, and predicted toxicity profiles, with compounds showing favorable pharmacokinetic properties, acceptable drug-likeness, and lower predicted toxicity considered higher-priority candidates for subsequent *in silico* analysis. Computational predictions were considered preliminary and were not interpreted as experimental evidence of efficacy or safety[24].

Cell viability and adipogenesis in 3T3-L1 cells

The cytotoxicity of the ethanolic extract of *O. umbellata* was evaluated using the MTT assay. The mouse preadipocyte cell line (3T3-L1 passage number PN11) was seeded in 96-well plates at a density of 1×10^4 cells/well in Dulbecco's Modified Eagle Medium (DMEM) supplemented with 10% fetal bovine serum (FBS) (Himedia, India) and 1X antibiotic-antimycotic solution. The cells were maintained at 37°C in a humidified incubator containing 5% CO_2. After reaching the appropriate confluence, the cells were washed with 200 µL of 1X phosphate-buffered saline (PBS) and treated with different concentrations of *O. umbellata* extract (25, 50, 100, 250, and 500 µg/ mL) prepared in serum-free medium. 35% DMSO was used as the positive control, while untreated cells served as the control group. The cells were incubated with the respective treatments for 24 h. Following treatment, the medium was aspirated, and 0.5 mg/ mL MTT solution prepared in 1X PBS was added to each well and incubated at 37°C for 4 h. The MTT-containing solution was then removed, and the cells were washed with 200 µL PBS. The resulting formazan crystals were dissolved in 100 µL DMSO and mixed thoroughly. Absorbance was measured at 570 nm using a microplate reader[25]. Cell viability was calculated as a percentage of the untreated control using the formula:

Cell viability (%) = [Absorbance of sample / Absorbance of control] × 100

Adipocyte differentiation of 3T3-L1 cells

Adipocyte differentiation of 3T3-L1 preadipocytes was performed following the previously published protocol with minor modifications[26]. Briefly, 3T3-L1 preadipocytes were seeded in 12-well plates at a density of 3×10^4 cells/well in DMEM supplemented with 10% FBS and maintained at 37°C in a humidified atmosphere containing 5% CO_2. After reaching 100% confluence, the cells were incubated for 24 h before induction of differentiation. The growth medium was then replaced with induction medium consisting of DMEM supplemented with 10% FBS, 0.5 mM 3-isobutyl-1-methylxanthine (IBMX), 1 µM dexamethasone, and 1.7 µM insulin, and the cells were incubated for 2 days. Subsequently, the induction medium was replaced with maintenance medium consisting of DMEM supplemented with 10% FBS and 1.7 µM insulin. The *O. umbellata* ethanolic extract was added at 100 µg/ mL, a concentration selected based on the cell viability assay, during the post-induction period. The treatment medium containing the extract was replaced every 2 days, and treatment was continued throughout the

8-day differentiation period. For comparison, the undifferentiated control consisted of 3T3-L1 cells maintained in growth medium without adipogenic induction or extract treatment, whereas the differentiated control consisted of cells subjected to the complete adipogenic differentiation protocol without *O. umbellata* extract treatment. The adipogenesis experiments were performed in three independent replicates. These controls were used to distinguish basal cellular characteristics from changes associated with adipogenic differentiation and extract treatment.

Oil red O staining and lipid quantification

Following the induction of differentiation, 3T3-L1 adipocytes were washed twice with phosphate-buffered saline (PBS) and fixed with 4% paraformaldehyde for 30 min at room temperature to preserve cellular morphology. The differentiated cells were treated with *O. umbellata* ethanolic extract at 100 µg/ mL during the adipogenesis period. After fixation, cells were washed again with PBS and stained with 0.3% Oil Red O solution, prepared in isopropanol and diluted with water (3:2), for 30 min to visualize intracellular lipid droplets indicative of adipogenesis[27]. Excess stain was removed by washing gently with distilled water until clear, and stained cells were observed under an inverted microscope to capture representative images of lipid accumulation. For quantification, the retained dye was eluted by adding 100% isopropanol to each well, and the absorbance was measured at 490 nm using a microplate reader, providing an estimate of the relative lipid content among treatment groups. The absorbance values were used as a measure of relative intracellular lipid accumulation among the treatment groups.

Triglyceride estimation

Intracellular triglyceride content was determined using a commercial triglyceride assay kit (COD 11828; BioSystems Diagnostics Pvt. Ltd., India). Following treatment, the cells were washed with phosphate-buffered saline (PBS) and homogenized using a homogenizing solution containing 154 mM KCl, 1 mM ethylenediaminetetraacetic acid (EDTA), and 50 mM Tris buffer (pH 7.4). The cell lysates were centrifuged at 3,000 rpm for 5 min to remove the fat layer, and the resulting supernatants were collected for triglyceride and total protein estimation. Triglyceride content was quantified using the enzymatic colorimetric method according to the manufacturer's instructions, while total protein content was determined using a commercial total protein assay kit (Cat. No. 1101201150; Coral Clinical Systems, India). The absorbance for triglyceride and total protein estimation was measured at 500 and 550 nm, respectively, using a double-beam UV/Vis spectrophotometer (LMSP-UV-1200-PC, Labman Scientifics, India). Triglyceride content was normalized to the corresponding total protein content and expressed as a relative measure of intracellular triglyceride accumulation[27,28].

Gene expression analysis by RT-qPCR

For gene expression analysis, total RNA was isolated from differentiated and *O. umbellata* treated 3T3-L1 adipocytes using TRIzol reagent (Ambion, USA) according to the manufacturer's protocol. The extracted RNA was quantified using a spectrophotometer, and 3 µg of total RNA was used for reverse transcription. Complementary DNA (cDNA) was synthesized using the PrimeScript™ 1st Strand cDNA Synthesis Kit (Takara Bio Inc., Japan) according to the manufacturer's instructions. The reverse-transcription reaction was performed in a final volume of 20 µL containing 3 µg of total RNA, 1 µL of oligo(dT) primer (50 µM), 1 µL of dNTP mixture (10 mM each), 4 µL of 5X PrimeScript Buffer, 0.5 µL of RNase inhibitor (40 U/µL), and 1 µL of PrimeScript RTase (200 U/µL), with DEPC-treated water added to make up the final volume. The reaction was incubated at 42°C for 60 min, followed by termination at 95°C for 5 min. One microliter of the resulting cDNA was used for quantitative real-time PCR (RT-qPCR)[28,29].

RT-qPCR was performed using AccuPower® 2X Greenstar™ qPCR Master Mix (Bioneer, South Korea) on a Rotor-Gene Q 2PLEX HRM Real-Time PCR system (Qiagen). Each PCR reaction was prepared in a final volume of 25 µL containing 12.5 µL of 2X qPCR Master Mix, gene-specific forward and reverse primers at a final concentration of 400 nM each and cDNA template. The amplification conditions consisted of enzyme activation at 50°C for 2 min and denaturation at 95°C for 15 min, followed by 40 cycles of denaturation at 95°C for 15 s and annealing/extension at 60°C for 30 s. GAPDH was used as the endogenous reference gene for normalization. Gene expression levels of FAS, SREBP-1c, PPARγ, leptin, and adiponectin were determined relative to GAPDH expression using the

Table 1 — Primer sequences used for qRT-PCR analysis

Gene	Forward primer (5′–3′)	Reverse primer (5′–3′)
FAS	CCCCTCTGTTAATTGGCTCC	TTGTGGAAGTGCAGGTTAGG
SREBP-1c	GTGAGCCTGACAAGCAATCA	GGTGCCTACAGAGCAAGAG
PPARγ	GCCAAGGCGAGGGCGATC	CACGGATCGAAACTGGCACC
Leptin	CAGCTGCAAGGTGCAAGAAG	GATACCGACTGCGTGTGTGA
Adiponectin	GATGCAGGTCTTCTTGGTCCT	ACATAAGCGGCTTCTCCAGG

2^−ΔΔCt method. Gene-expression data were summarized across the three independent experiments and expressed as mean ± SD. The primer sequences used for the selected genes are presented in (Table 1). Melt-curve analysis was performed following amplification to confirm the specificity of the PCR products.

Statistical analysis

All experiments were independently performed in triplicate (n = 3 independent experiments), and data are presented as mean ± standard deviation (SD), unless otherwise stated. Statistical differences among experimental groups were evaluated using one-way analysis of variance (ANOVA), followed by Tukey's multiple-comparison post hoc test. A p-value < 0.05 was considered statistically significant. For dose–response experiments, IC_{50} values were estimated by nonlinear regression analysis using an appropriate dose–response model, with 95% confidence intervals (CIs). Exact p-values were reported where available.

Results and Discussion

Plant collection and authentication

Fresh whole plants of *O. umbellata* were collected and authenticated as *Oldenlandia umbellata* L. (Rubiaceae) by Dr. S. Mutheeswaran, with voucher specimen number XCH 40509 (Fig. 1). In contrast, powdered *D. ebenum* bark was procured from a local herbal supplier; the use of commercially sourced *D. ebenum* material was necessitated by the limited availability of fresh material and associated conservation considerations[30].

Preparation of plant extracts

The plant materials were extracted using solvents of different polarities, namely petroleum ether, ethyl acetate, ethanol, and water, to facilitate the recovery of diverse classes of phytoconstituents. The powdered plant material was subjected to maceration in the respective solvents for 72 h, followed by filtration and concentration of the extracts. The ethanolic extracts yielded 0.85 g (1.70%) from *D. ebenum* and 0.93 g (1.86%) from *O. umbellata*, based on 50 g of dried



Fig. 1 — Taxonomically authenticated plant specimen of *O. umbellata*

powdered plant material. Among the extracts obtained, the ethanolic extracts exhibited comparatively broader qualitative phytochemical profiles and were therefore selected for subsequent studies. The broader phytochemical profile observed in the ethanolic extracts may be related to the ability of ethanol to extract a relatively diverse range of phytoconstituents with varying polarity characteristics.

Preliminary phytochemical screening

Preliminary qualitative phytochemical screening revealed clear variation in the phytochemical profiles of the extracts depending on the solvent used. The ethanolic extract of *O. umbellata* showed the presence of alkaloids, carbohydrates, steroids, proteins, flavonoids, and phenols, whereas the ethanolic extract of *D. ebenum* contained alkaloids, carbohydrates, steroids, proteins, triterpenoids, phenols, and tannins. Compared with the other solvent extracts, the ethanolic extracts displayed a broader range of detected phytochemical groups in both plant species. Based on this qualitative phytochemical profile, the ethanolic extracts were prioritized for subsequent biological evaluation.

The solvent-dependent differences observed in (Table 2) indicate that extraction polarity influenced

Table 2 — Preliminary qualitative phytochemical analysis of *D. ebenum* and *O. umbellata*

Solvent	Alkaloids	Carbohydrates	Steroids	Proteins	Flavonoids	Triterpenoids	Phenols	Tannins	Saponins
				O. umbellata					
Petroleum ether	+	+	+	+	+	–	+	–	–
Ethyl acetate	–	+	+	–	+	–	+	–	–
Water	+	+	–	+	+	–	+	–	+
Ethanol	+	+	+	+	+	–	+	–	–
				D. ebenum					
Petroleum ether	–	–	+	–	–	+	–	–	–
Ethyl acetate	–	–	+	–	–	+	+	+	–
Water	+	+	–	+	–	–	+	+	+
Ethanol	+	+	+	+	–	+	+	+	+

the recovery of different classes of phytoconstituents. These findings provided a preliminary basis for selecting the ethanolic extracts for the subsequent enzyme inhibition and anti-adipogenic investigations.

Cytotoxicity evaluation on Vero cells

Vero cells were utilized as a non-cancerous mammalian cell model to establish the preliminary safety profile and non-toxic working concentration range of the plant extracts. The cytotoxic effects of the ethanolic extracts of *D. ebenum* and *O. umbellata* were evaluated using the MTT cell viability assay across concentrations ranging from 100 to 500 µg/mL following 24 h of treatment (Fig. 2a).

Both extracts demonstrated a concentration-dependent reduction in cell viability ($F(4,20) = 248.65$, $P < 0.0001$). At the lowest concentration tested (100 µg/mL), cell viability remained high at 90.40±1.82% for *D. ebenum* and 90.00±2.15% for *O. umbellata*, indicating minimal cytotoxicity (<10% toxicity). Non-linear regression analysis (4-parameter logistic curve fit) yielded half-maximal inhibitory concentration (IC_{50}) values of 396.43 µg/mL (95% CI: 381.12−412.35 µg/mL; R2=0.9912) for *D. ebenum* and 293.19 µg/mL (95% CI: 279.45−307.62 µg/mL; R2=0.9948) for *O. umbellata*. Two-way ANOVA with Tukey's post-hoc multiple comparisons revealed no statistically significant difference in cell viability between the two extracts at 100 µg/mL ($P = 0.9840$) or 200 µg/mL ($P = 0.2450$). However, at higher concentrations (≥300 µg/mL), *O. umbellata* induced significantly greater cytotoxicity than *D. ebenum* ($P < 0.0001$).

Microscopic examination at 100× magnification (Fig. 2b-d) corroborated the quantitative MTT findings. Following 24 h of treatment with 100 µg/mL extract, cells maintained normal monolayer morphology without evidence of overt cellular

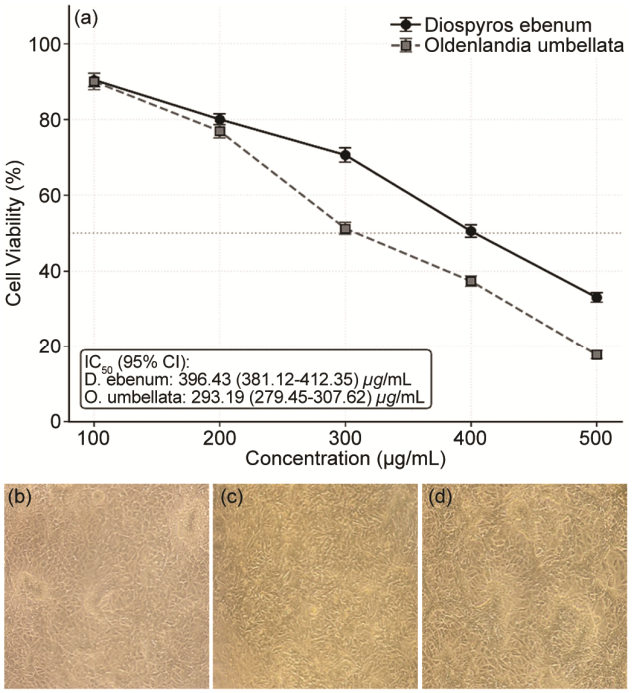


Fig. 2 — *In vitro* cytotoxicity and cellular morphological assessment in Vero mammalian cells. (a) Concentration-dependent cell viability profile of Vero cells following 24 h treatment with *D. ebenum* and *O. umbellata* ethanolic extracts. Representative phase-contrast micrographs (100× magnification) displaying cellular morphology after 24 h; (b) untreated control; (c) *D. ebenum* treated cells; and (d) *O. umbellata* treated cells

distress, such as cell shrinkage, cytoplasmic vacuolation, membrane blebbing, or detachment. Consequently, 100 µg/mL was identified as a non-toxic, biologically safe concentration under the tested conditions and selected for downstream functional cell studies.

***In vitro* enzyme inhibition**

The inhibitory effects of the ethanolic extracts of *D. ebenum* and *O. umbellata* against three enzymes

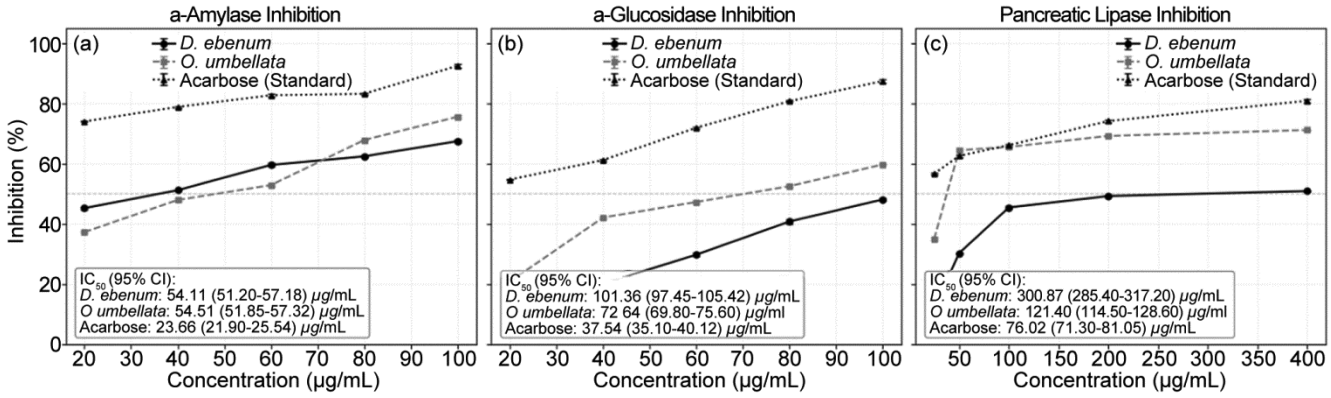


Fig. 3 — *In vitro* enzyme inhibitory profiles of *D. ebenum* and *O. umbellata* extracts. Percentage inhibition of (a) α-amylase; (b) α-glucosidase; and (c) pancreatic lipase across indicated concentrations compared with reference standards (Acarbose/Orlistat). Values are expressed as Mean ±SD (n=3). IC_{50} values and 95% confidence intervals (95% CI) were determined *via* 4-parameter logistic non-linear regression. Horizontal dashed lines represent 50% inhibition

relevant to carbohydrate and lipid digestion porcine pancreatic α-amylase, yeast α-glucosidase, and porcine pancreatic lipase were evaluated at different concentrations. Acarbose was used as the reference inhibitor for α-amylase and α-glucosidase, whereas orlistat was used as the reference inhibitor for pancreatic lipase (Fig. 3).

α-amylase inhibition

Both plant extracts demonstrated concentration-dependent inhibition of α-amylase activity across the tested range (20–100 µg/mL) (Fig 3A). Non-linear regression curve fitting (4-parameter logistic model) yielded half-maximal inhibitory concentration (IC_{50}) values of 54.11 µg/mL (95% CI: 51.20–57.18 µg/mL; R2=0.9841) for *D. ebenum*, 54.51 µg/mL(95% CI: 51.85–57.32 µg/mL; R2=0.9952) for *O. umbellata*, and 23.66 µg/mL (95% CI: 21.90–25.54 µg/mL; R2=0.9912) for Acarbose (Fig. 3a). One-way ANOVA revealed statistically significant variance in inhibitory potency across treatment groups ($F(2,6)=214.35$,$P<0.0001$). Post-hoc pairwise comparisons using Tukey's HSD test indicated no statistically significant difference in α-amylase inhibitory potency between *D. ebenum* and *O. umbellata* ($P = 0.9820$), demonstrating that both extracts possess equivalent, moderate amylase suppression. However, the commercial standard Acarbose exhibited significantly greater potency than both plant extracts ($P< 0.0001$).

Yeast α-glucosidase inhibition

The extracts exhibited marked dose-dependent inhibition of α-glucosidase activity (20–100 µg/mL), with *O. umbellata* displaying a substantially stronger concentration-response profile compared to *D. ebenum* (Fig 3b). The calculated IC_{50} values were 101.36 µg/mL (95% CI: 97.45–105.42 µg/mL; R2=0.9981) for *D. ebenum*, 72.64 µg/mL (95% CI: 69.80–75.60 µg/mL; R2=0.9945) for *O. umbellata*, and 37.54 µg/mL (95% CI: 35.10–40.12 µg/mL; R2=0.9934) for Acarbose. One-way ANOVA confirmed highly significant differences among the groups ($F(2,6)=482.19$, $P< 0.0001$). Tukey's post-hoc analysis demonstrated that the IC_{50} of *O. umbellata* was significantly lower than that of *D. ebenum* ($P<0.0001$), confirming its superior potency in suppressing α-glucosidase, though Acarbose remained the most potent overall ($P< 0.0001$).

Pancreatic lipase inhibition

Evaluation of pancreatic lipase suppression over a concentration range of 25–400 µg/mL revealed pronounced differences in efficacy (Fig. 3c). *O. umbellata* produced strong, concentration-dependent suppression with an IC_{50} of 121.40 µg/mL (95% CI: 114.50–128.60 µg/mL; R2=0.9854). In contrast, *D. ebenum* exhibited limited efficacy at higher concentrations, yielding an IC_{50} of 300.87 µg/mL (95% CI: 285.40–317.20 µg/mL; R2=0.9892). The reference inhibitor Orlistat exhibited an IC_{50} of 76.02 µg/mL (95% CI: 71.30–81.05 µg/mL; R2=0.9881). One-way ANOVA indicated a highly significant difference in lipase inhibition across treatments ($F(2,6)=356.81$, $P<0.0001$). Tukey's multiple comparison test confirmed that *O. umbellata* possessed significantly higher lipase inhibitory activity than *D. ebenum* ($P< 0.0001$), requiring less than half the concentration to achieve 50% enzyme inhibition.

Taken together, the comparative analysis of IC_{50} values and 95% confidence intervals revealed distinct biological profiles between the two plant species. While both *D. ebenum* and *O. umbellata* exhibited equivalent, moderate α-amylase inhibitory activity, *O. umbellata* displayed significantly higher dual inhibitory potency against both α-glucosidase ($P< 0.0001$) and pancreatic lipase ($P< 0.0001$).

In clinical pharmacology, a metabolic regulatory agent that combines strong α-glucosidase and pancreatic lipase inhibition with moderate α-amylase activity is highly advantageous, as excessive pancreatic amylase inhibition often causes uncomfortable abdominal distension, flatulence, and diarrhea due to unhydrolyzed starch fermentation in the colon. Given its superior multi-target inhibitory potency across lipid and carbohydrate digestive pathways, *O. umbellata* was prioritized and selected for downstream cellular investigations in 3T3-L1 pre-adipocytes to evaluate its anti-adipogenic and intracellular lipid-modulating potential. However, while these *in vitro* multi-enzyme inhibition results demonstrate significant bioactivity, they serve primarily as a mechanistic screening tool. In agreement with computational ADME predictions, these enzymatic assays alone do not directly confirm systemic bioavailability or clinical therapeutic efficacy, necessitating the further cellular, qRT-PCR, and metabolic investigations described below.

Information specifically addressing the inhibitory effects of *D. ebenum* and *O. umbellata* against α-amylase, α-glucosidase, and pancreatic lipase appears to be limited. However, related species belonging to the *Diospyros* and *Oldenlandia* genera have demonstrated a range of biological activities relevant to metabolic and inflammatory disorders. *D. kaki* has been reported to possess antioxidant and antidiabetic activities and has also demonstrated pancreatic lipase inhibitory activity, suggesting potential relevance to metabolic regulation[31]. *D. mespiliformis* has been associated with effects on cholesterol metabolism, type 2 diabetes, body weight, and α-glucosidase inhibition[32]. Similarly, *D. malabarica* has demonstrated anti-inflammatory effects *in vivo* through modulation of inflammatory markers, while *D. lotus* has been reported to reduce body weight and lipid and triglyceride accumulation in adipocytes. *D. peregrina* has also demonstrated antidiabetic activity in experimental models[33].

Related species of the genus *Oldenlandia* have likewise exhibited diverse pharmacological activities. *O.corymbosa* has been reported to possess hypoglycemic, antidiabetic, and antihyperlipidemic effects, while *O.diffusa* has demonstrated anti-inflammatory and antidiabetic effects in experimental studies and shown antiplasmodial activity, whereas compounds isolated from *O.hedyotidea* have demonstrated anticancer activity[34,35]. *O.auricularia* has also been traditionally used for the management of hypertension, with experimental observations indicating no apparent detrimental effects on liver and kidney function.

Although these reports concern different species, they provide a broader context for the pharmacological potential of the two genera and support further investigation of *D. ebenum* and *O. umbellata*. The comparatively stronger enzyme inhibitory activity observed for *O. umbellata* in the present study, particularly against α-glucosidase and pancreatic lipase, provides a rationale for its further evaluation in the subsequent cellular experiments. The observed activity should nevertheless be interpreted as preliminary *in vitro* evidence rather than direct evidence of anti-obesity or therapeutic efficacy.

GC–MS analysis of *O. umbellata*

As *O. umbellata* showed comparatively stronger inhibitory activity in the preceding enzyme assays, its ethanolic extract was further investigated by GC-MS to characterize its putatively identified phytochemical constituents. The GC-MS chromatogram of the *O. umbellata ethanolic* extract is shown in (Fig. 4).

GC-MS analysis revealed several compounds that have previously been associated with diverse biological activities. Hexadecanamide (RT: 16.63 min) has been reported to possess anti-inflammatory activity, including effects associated with mast cell activation and inflammatory mediators, and has been investigated in the context of Staphylococcus aureus-induced mastitis. Flavone (RT: 16.03 min) has also been reported to exhibit antioxidant activity and has been associated with inhibition of digestive enzymes such as α-amylase and pancreatic lipase. Octadec-9-enoic acid (oleic acid; RT: 18.38 min) has been investigated for its potential role in regulating circadian rhythm-associated genes in adipose tissue. Alterations in adipose circadian regulation have been associated with metabolic dysfunction, and the reported effects of oleic acid on lipid metabolism and inflammatory processes provide a possible mechanistic context for its relevance to metabolic health.

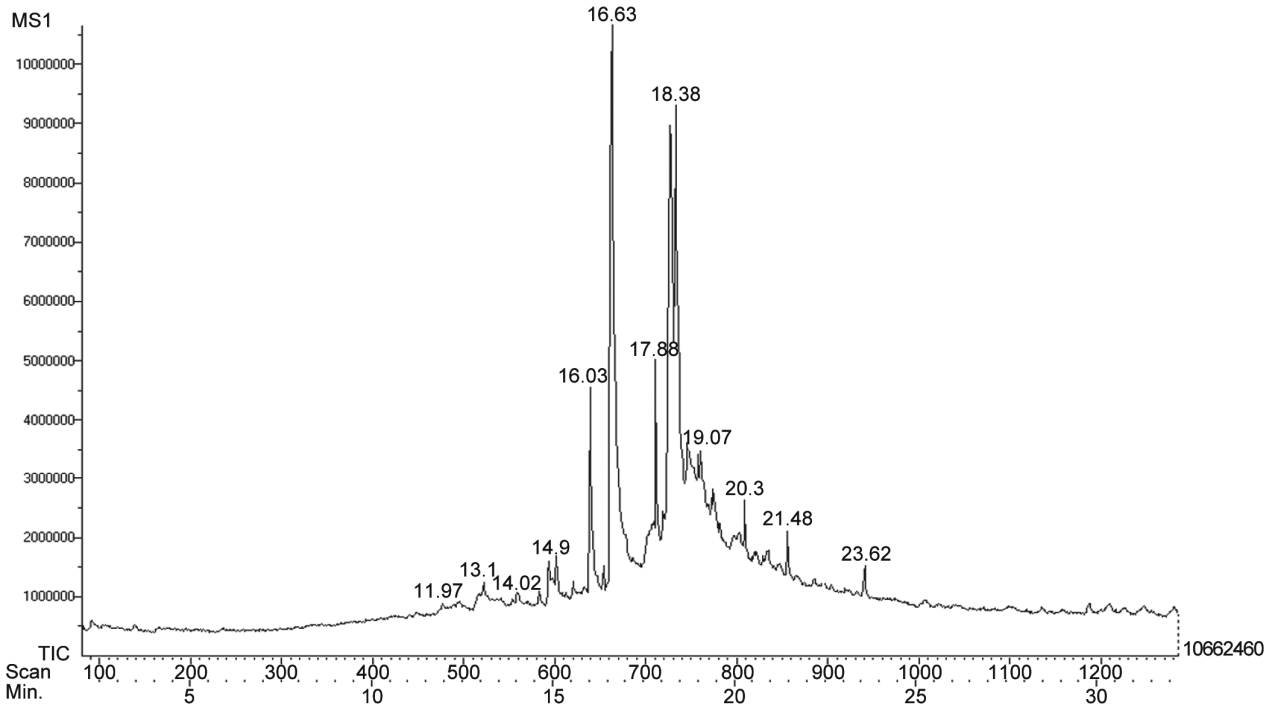


Fig. 4 — GC-MS chromatogram of *O. umbellata* ethanolic extract

Coumarin, 3-(2-(1-methyl-2-imidazolylthio)-1-oxoethyl)- (RT: 21.48 min), a coumarin derivative, has been associated with several biological activities, including anti-inflammatory, anticoagulant, anticancer, and antimicrobial effects. In addition, p-coumaric acid, a structurally related phenolic compound, has been reported to attenuate metabolic syndrome in experimental mouse models through activation of brown adipose tissue and increased expression of uncoupling protein 1 (UCP1), thereby promoting thermogenesis and energy expenditure[36].

Collectively, these reports indicate that several compounds putatively identified in the *O. umbellata* extract have previously been associated with biological processes relevant to inflammation, lipid metabolism, oxidative stress, and energy homeostasis. However, the presence of a compound in a GC-MS profile does not by itself establish that the compound is responsible for the biological activity observed in the present study.

***In silico* ADME and toxicity prediction**

The identified compounds through GC-MS were subsequently subjected to *in silico* analysis. The physicochemical, pharmacokinetic, drug-likeness, and toxicity profiles of the compounds identified by GC-MS, together with selected compounds obtained from literature and database searches, were evaluated using SwissADME, Osiris and ProTox-3.0 and the detailed results are provided in (Suppl. Tables S1 and S2). Of the 28 compounds evaluated, 14 exhibited physicochemical and predicted ADME characteristics compatible with commonly applied drug-likeness criteria, including Lipinski's rule of five. Among the 14 compounds that satisfied the initial physicochemical and ADME-based screening criteria, Osiris toxicity prediction was subsequently performed to further assess their predicted safety profiles. Based on the Osiris analysis, 8 compounds ursolic acid, deacetylasperuloside, nicotinic acid, hexadecanamide, cyclopentanetridecanoic acid methyl ester, octadec-9-enoic acid, pyrimidine, 5-ethyl-2-[4-(4-ethylcyclohexyl)phenyl]-, and glucose showed no predicted adverse effects in the evaluated toxicity endpoints. These eight compounds were therefore retained for further *in silico* toxicity assessment and subsequent screening. These eight compounds were further evaluated using ProTox-3.0, and all showed predicted toxicity classes ranging from Class IV to Class VI, thereby satisfying the predefined toxicity-screening criterion and supporting their retention for subsequent *in silico* lead identification.

These predictions were used as a prioritization step to identify compounds with comparatively favorable computational ADME characteristics for further

investigation rather than as evidence of confirmed oral bioavailability or therapeutic efficacy. Ursolic acid has been extensively investigated for its potential anti-obesity effects and has been reported to influence adipocyte differentiation, lipid accumulation, inflammation, and metabolic dysfunction in experimental models[37]. Nicotiflorin has been associated with anti-inflammatory and antioxidant activities, in addition to several other reported pharmacological effects, and has been identified in medicinal plants traditionally used in Chinese medicine[38]. Anthraquinone derivatives have also been investigated for antioxidant, metabolic, and lipid-modulating activities, supporting their potential relevance to metabolic health. β-Sitosterol has been reported to influence lipid metabolism and cholesterol absorption and possesses antioxidant properties. Among the compounds identified or considered in the present analysis, flavone has been associated with lipid metabolism regulation[39], whereas octadec-9-enoic acid has been implicated in fatty acid metabolism and oxidation. The combination of these reported biological activities with the favorable predicted ADME characteristics observed for a subset of the evaluated compounds provides a basis for prioritizing selected *O. umbellata* constituents for subsequent experimental investigation.

Nevertheless, the predicted pharmacokinetic and toxicity properties should be interpreted as computational estimates, and experimental studies are required to confirm compound identity, bioavailability, cellular activity, and safety. The observed enzyme inhibitory and subsequent cellular effects therefore cannot be attributed to any individual GC-MS-identified compound without further isolation, characterization, and validation.

Assessment of cell viability on 3T3-L1 adipocytes

The effect of *O. umbellata* ethanolic extract on 3T3-L1 cell viability was evaluated at concentrations

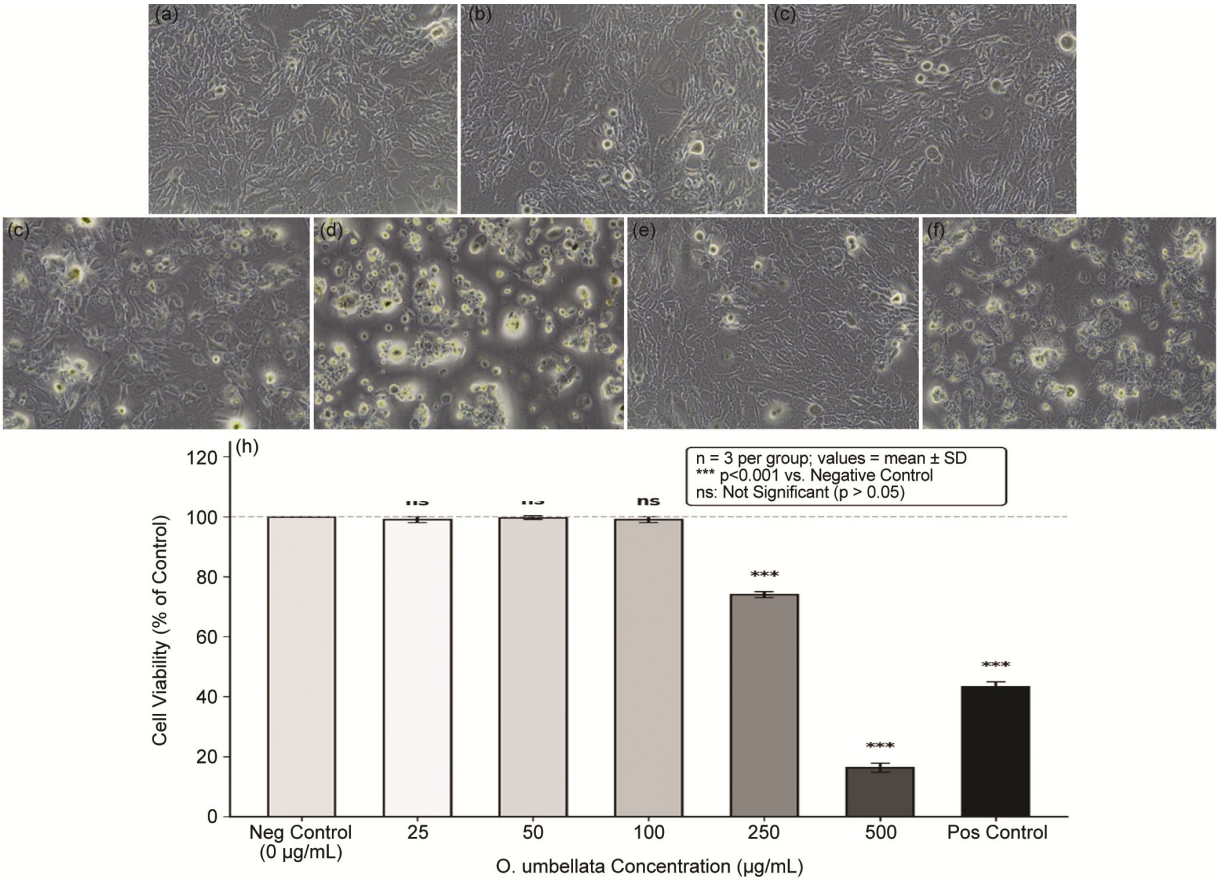


Fig. 5 — Effect of *O. umbellata* extract on the morphology and viability of 3T3-L1 preadipocytes. (a–g) Phase-contrast microscopic images showing cellular morphology following 24 h treatment: (a) untreated negative control 0 µg/mL; (b) 25 µg/mL; (c) 50 µg/mL; (d) 100 µg/mL; (e) 250 µg/mL; (f) 500 µg/mL; (g) positive control; and (h) Quantitative cell viability assessed *via* MTT assay across increasing concentrations of *O. umbellata* (25 - 500 µg/mL). Data are expressed as mean ± SD (n = 3 independent experiments per group). Statistical significance relative to the negative control: $^{***}P < 0.001$; ns indicates non-significant difference ($P > 0.05$)

ranging from 25 to 500 µg/ mL using the MTT assay. All treatments were performed in triplicate (n=3), and the results are presented as mean ± SD (Fig. 5). Cell viability remained high at 25, 50, and 100 µg/ mL, with mean viabilities of 99.00 ±1.00%, 99.67 ± 0.58%, and 99.00 ± 1.00%, respectively, compared with 100.00 ± 0.00% for the untreated negative control. In contrast, viability markedly decreased to 74.00 ± 1.00% at 250 µg/ mL and 16.33 ± 1.53% at 500 µg/ mL, indicating a concentration-dependent loss of cell viability at higher doses. One-way ANOVA demonstrated a highly significant difference among treatment groups ($F(6,14)=2986.06$, $P = 6.36 \times 10^{-21}$, $\eta p^2=0.999$). Tukey's HSD post-hoc analysis confirmed that the 25, 50, and 100 µg/ mL groups did not differ significantly from the negative control (P = 0.903–1.000), whereas viability at 250 and 500 µg/ mL was significantly lower than that of both the negative control ($P< 0.001$) and the 100 µg/ mL group ($P< 0.001$). Non-linear regression analysis (four-parameter logistic curve fit) revealed the half-maximal inhibitory concentration (IC_{50}) of the *O. umbellata* extract to be 311.2 µg/ mL (95% CI: 301.5–321.4 µg/ mL; $R^2=0.996$).

These findings indicate that concentrations up to 100 µg/ mL maintain cell viability without non-specific cytotoxicity. Consequently, 100 µg/ mL was selected as the maximum non-toxic working concentration for subsequent anti-adipogenic assays. Selecting a non-cytotoxic dose ensures that observed reductions in lipid accumulation, intracellular triglyceride levels, or adipogenic gene expression stem from specific bioactivity rather than compromised cell viability.

Inhibitory effect of *O. umbellata* on lipid accumulation in 3T3-L1 cells

Oil Red O staining was used to evaluate intracellular lipid accumulation in differentiated 3T3-L1 adipocytes, a standard quantitative and visual method for assessing adipogenesis[40]. Following treatment with 100 µg/ mL of the ethanolic extract of *O. umbellata*, lipid accumulation was evaluated microscopically and quantified spectrophotometrically by measuring the absorbance of eluted Oil Red O dye at 490 nm.

Microscopic examination revealed a marked reduction in intracellular lipid droplet size and density

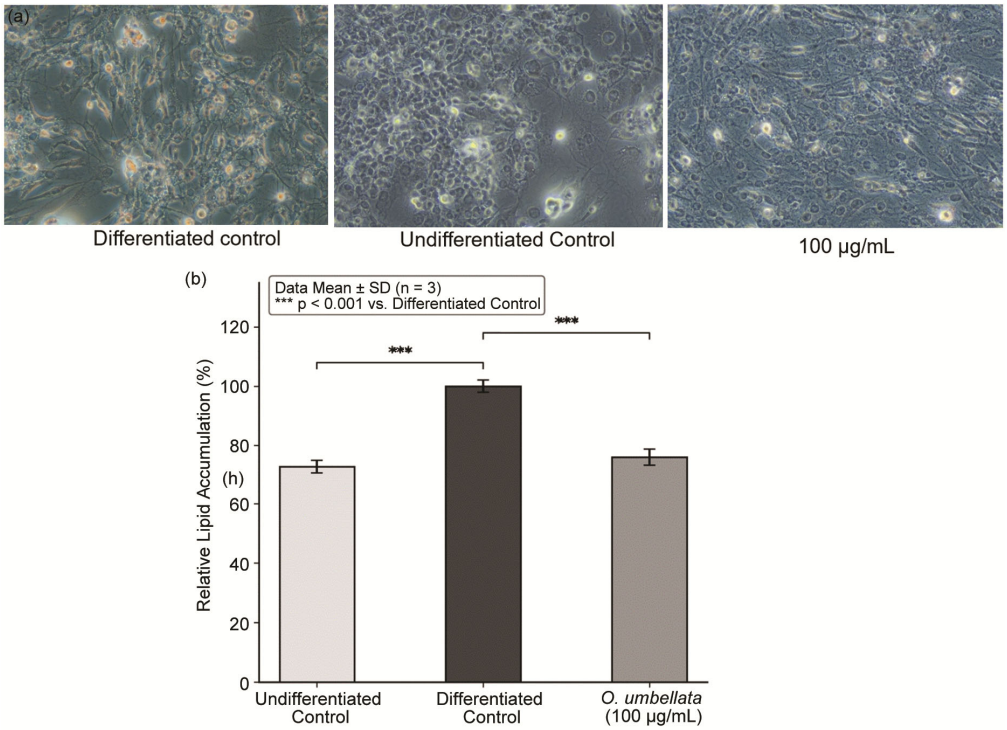


Fig. 6 — Effect of *O. umbellata* extract on intracellular lipid accumulation in 3T3-L1 adipocytes. (a) Representative phase-contrast microscopic images showing cellular morphology and lipid droplet accumulation in differentiated control (left), undifferentiated control (middle), and *O. umbellata*-treated (100 µg/mL) differentiated adipocytes (right); and (b) Quantitative analysis of relative lipid accumulation expressed as a percentage of the differentiated control group. Data are presented as mean ± SD (n=3 independent experiments). Statistical significance relative to the differentiated control:***$P< 0.001$

in the *O. umbellata* treated group compared with the fully differentiated control group (Fig. 6). The lipid accumulation pattern in treated cells was visually comparable to that of undifferentiated preadipocytes. Importantly, this anti-adipogenic effect occurred at a concentration (100 µg/ mL) that demonstrated no cytotoxic effects in the preceding cell viability assay (>99% cell viability).

Quantitative spectrophotometric analysis confirmed the microscopic findings. Absorbance values at 490 nm were 0.737 ± 0.015 for the differentiated control, 0.537 ± 0.015 for the undifferentiated control, and 0.560 ± 0.020 for the *O. umbellata* treated group (100 µg/ mL). Treatment with 100 µg/ mL *O. umbellata significantly* reduced intracellular lipid accumulation by 23.98% relative to the differentiated control (76.02 ± 2.71% vs. 100.00 ± 2.07%, $P< 0.001$). One-way ANOVA demonstrated a highly significant difference in lipid accumulation among the groups ($F(2,6)=117.43$, $P = 1.34 \times 10^{-5}$, partial eta-squared=0.975). Tukey's HSD post-hoc analysis confirmed that the differentiated control group accumulated significantly more lipid than both the undifferentiated control ($P< 0.0001$) and the *O. umbellata* treated group ($P = 0.0001$). Furthermore, no statistically significant difference was observed between the *O. umbellata*-treated group and the undifferentiated control group ($P = 0.283$), indicating that 100 µg/ mL *O. umbellata effectively* suppressed lipid accumulation to levels near baseline preadipocyte levels.

The reduction in intracellular lipid accumulation observed following *O. umbellata* treatment suggests that the extract may interfere with lipid deposition during 3T3-L1 adipocyte differentiation. Because Oil Red O staining primarily measures accumulated neutral lipids, these results alone do not establish whether the extract inhibits adipocyte differentiation, lipid synthesis, or both. Additional measurements of intracellular triglycerides and adipogenesis-related gene expression were therefore performed to further investigate the effect of the extract and its possible molecular basis.

The observed reduction in lipid accumulation is consistent with previous reports describing the ability of natural compounds to modulate adipocyte differentiation and lipid deposition[41]. Effective anti-obesogenic strategies may involve modulation of adipocyte differentiation and lipid accumulation, rather than relying solely on reduction of cell number. Inhibition of adipogenesis and modulation of adipocyte survival have also been proposed as potential approaches for limiting adipose tissue expansion.

Taken together, the present findings provide preliminary evidence that *O. umbellata may* possess anti-adipogenic potential by reducing lipid accumulation in differentiated 3T3-L1 cells without substantial cytotoxicity at the concentration tested. Further assessment of intracellular triglyceride content and adipogenesis-associated molecular markers is necessary to determine whether the observed effect is accompanied by changes in lipid metabolism and adipogenic regulatory pathways.

Assessment of intracellular triglyceride levels

Adipocyte differentiation is accompanied by increased lipid storage and intracellular triglyceride accumulation, processes that contribute to adipose tissue expansion and metabolic dysfunction. Triglycerides represent the major form of stored lipid in adipocytes and are mobilized as fatty acids according to cellular energy requirements. Alterations in triglyceride synthesis and lipid metabolism have also been associated with obesity and hyperlipidemia in experimental models, supporting the investigation of triglyceride accumulation as an indicator of adipocyte lipid storage.

In the present study, intracellular triglyceride levels were measured in 3T3-L1 cells following treatment with *O. umbellata extract* at 100 µg/ mL (n=3; Fig. 7). The undifferentiated control group exhibited a low baseline triglyceride content of 0.046 ± 0.001 mg/mg protein, whereas induction of differentiation markedly increased intracellular triglyceride accumulation to 0.341±0.002 mg/mg protein in the differentiated control group. Treatment with 100 µg/ mL *O. umbellata* extract significantly reduced intracellular triglyceride content to 0.188 ± 0.004 mg/mg protein, representing a 44.72% suppression in triglyceride accumulation compared with the differentiated control (55.28 ± 1.03% vs. 100.00 ± 0.61%).

One-way ANOVA demonstrated a highly significant difference in intracellular triglyceride levels among the treatment groups ($F(2,6)=11333.12$, $P = 1.62 \times 10^{-11}$, partial eta-squared=0.9997). Tukey's HSD post-hoc analysis revealed that the differentiated control group accumulated significantly higher triglyceride levels than both the undifferentiated control group

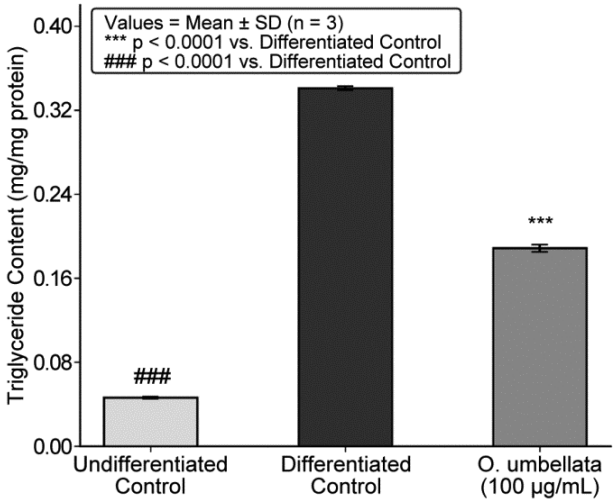


Fig. 7 — Inhibition of intracellular triglyceride accumulation by *O. umbellata* ethanolic extract in 3T3-L1 adipocytes. Intracellular triglyceride content was measured on day 8 of differentiation and normalized to total cellular protein (mg/mg protein). Data are presented as mean ± SD (n = 3). Differences between treatment groups were evaluated using one-way ANOVA followed by Tukey's HSD post-hoc test (***$P < 0.0001$). Treatment with 100 µg/mL O. umbellata significantly reduced intracellular triglyceride accumulation by 44.72% compared to the differentiated control ($P < 0.0001$)

(P<0.0001) and the *O. umbellata* treated group (P<0.0001). Furthermore, the triglyceride content in the *O. umbellata* treated group remained significantly higher than that in the undifferentiated control group (P< 0.0001), indicating a strong partial suppression of adipogenic lipid loading.

The reduction in intracellular triglyceride accumulation following *O. umbellata treatment* supports the finding that the extract attenuated lipid storage during 3T3-L1 adipocyte differentiation. Because triglyceride accumulation is an important hallmark of adipocyte maturation, these findings provide clear evidence for the anti-adipogenic potential of the extract. However, triglyceride quantification alone cannot establish the specific molecular mechanism responsible for this reduction; these results should therefore be interpreted in conjunction with the Oil Red O staining and downstream gene-expression analyses. To our knowledge, the present findings provide preliminary evidence for the lipid-lowering effect of *O. umbellata in* a 3T3-L1 adipocyte model. Further molecular analyses are required to determine whether the reduction in triglyceride accumulation is associated with modulation of key transcriptional regulators of adipogenesis and lipogenesis.

Expression of key markers associated with adipogenesis in 3T3-L1 Cells

Adipogenesis is a complex cellular process involving coordinated changes in transcription factors, lipid-synthesis enzymes, and adipocyte-derived regulatory molecules that control adipocyte differentiation and lipid storage. To investigate the molecular basis underlying the effects of *O. umbellata*, the expression of selected adipogenesis and lipid metabolism associated genes was examined by qRT-PCR. The genes analyzed included PPARγ, SREBP-1c, FAS, adiponectin, and leptin, and the corresponding primer sequences are provided in (Table 1).

PPARγ is a major transcriptional regulator of adipocyte differentiation and promotes the expression of genes involved in lipid uptake, fatty acid metabolism, and triglyceride storage. SREBP-1c regulates de novo fatty acid synthesis, including transcriptional regulation of FAS, an enzyme involved in fatty acid biosynthesis. Adiponectin is an adipocyte-derived hormone associated with lipid metabolism and insulin sensitivity, whereas leptin contributes to regulation of energy homeostasis. Therefore, changes in the expression of these genes were examined to determine whether *O. umbellata* treatment was associated with alterations in adipogenic differentiation and lipid metabolism.

Gene-expression analysis

Treatment of differentiated 3T3-L1 adipocytes with *O. umbellata* extract (100 μg/ mL) resulted in significant alterations in the mRNA expression of key adipogenesis-associated regulatory genes following normalization to the housekeeping gene GAPDH (Fig. 8; n=3 independent experiments). One-way ANOVA demonstrated highly significant overall treatment effects across all five evaluated genes: FAS [$F(2,6)=21399.70$,$P<$ 0.0001], PPARγ [$F(2,6)=1489.14$,$P<0.0001$],SREBP1c[$F(2,6)=548.88$, $P<$ 0.0001], Leptin [$F(2,6)=7858.74$, $P<$ 0.0001], and Adiponectin[$F(2,6)=28842.25$, $P<$ 0.0001]. Pairwise post-hoc evaluations using Tukey's HSD test revealed specific transcriptomic shifts (Table 3).

Values represent pairwise comparisons derived from one-way Analysis of Variance (ANOVA) followed by Tukey's post-hoc test ($n = 3$ independent experiments per group). Significance notation: *$P<$ 0.05, ** $P<$ 0.01, and *** $P<$ 0.001; ns indicates a non-significant difference ($P>$ 0.05).

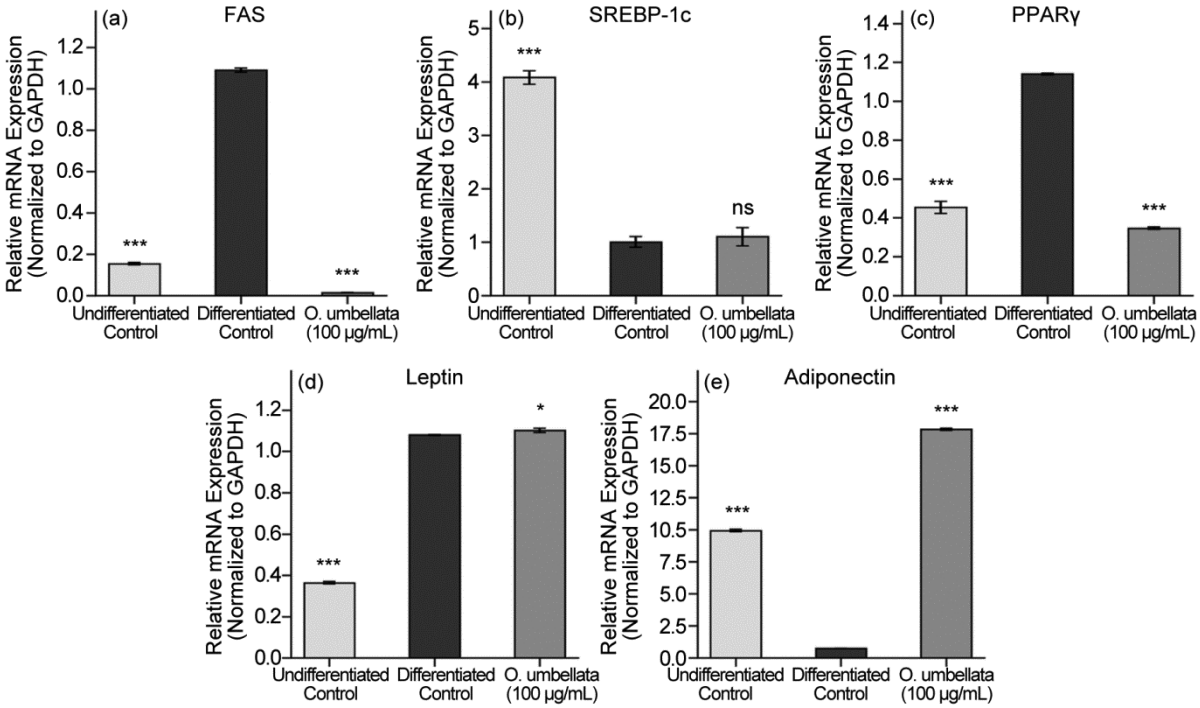


Fig. 8 — Effect of *O. umbellata* extract on adipogenesis-associated gene expression in 3T3-L1 cells. Relative mRNA expression of (a) FAS; (b) SREBP-1c; (c) PPARγ; (d) Leptin; and (e) Adiponectin quantified *via* qRT-PCR on day 8 of differentiation and normalized to GAPDH. Data represent mean ± SD (n = 3). Statistical significance was determined by one-way ANOVA with Tukey's HSD post-hoc test **P*< 0.05, ***P*< 0.01, **P*< 0.001, ns = not significant vs. differentiated control). Treatment (100 µg/mL) significantly downregulated FAS and PPARγ ($P < 0.0001$) while upregulating Adiponectin ($P < 0.0001$)

Table 3 — Pairwise post-hoc statistical comparisons (Tukey's HSD) of adipogenesis-associated gene expression in 3T3-L1 cells

Gene	Differentiated Control vs. Undifferentiated Control	Differentiated Control vs. *O. umbellata* Treated	Undifferentiated Control vs. *O. umbellata* Treated	Overall ANOVA (F-statistic, df)
FAS	***P< 0.0001	***P< 0.0001	***P = 0.0002	F(2, 6) = 21399.70, P< 0.0001
SREBP-1c	***P< 0.0001	P = 0.6120 (ns)	***P< 0.0001	F(2, 6) = 548.88, P< 0.0001
PPARγ	***P< 0.0001	***P< 0.0001	**P = 0.0016	F(2, 6) = 1489.14, P< 0.0001
Leptin	***P< 0.0001	P = 0.0270*	***P< 0.0001	F(2, 6) = 7858.74, P< 0.0001
Adiponectin	***P< 0.0001	***P< 0.0001	***P< 0.0001	F(2, 6) = 28842.25, P< 0.0001

FAS expression was markedly suppressed in the *O. umbellata*-treated group (0.014±0.001-fold) compared to both the differentiated control (1.090 ± 0.010-fold, P< 0.0001) and undifferentiated control groups (0.154±0.006-fold, P = 0.0002). This reduction is consistent with decreased expression of a key enzyme involved in *de novo* fatty acid synthesis and may contribute to reduced intracellular triglyceride levels and lipid droplet accumulation observed in the treatment group.

PPARγ expression was significantly lower in the *O. umbellata*-treated group (0.347 ± 0.006-fold) than in the differentiated control (1.140 ± 0.005-fold, P< 0.0001) and undifferentiated preadipocyte control (0.453 ± 0.031-fold, P =0.0016). The suppression of PPARγ the master transcriptional regulator of adipogenesis indicates that *O. umbellata* attenuates the central transcriptional network governing preadipocyte differentiation into mature fat-storing cells.

Sterol Regulatory Element-Binding Protein 1c (SREBP-1c) expression differed significantly between undifferentiated preadipocytes (4.083 ± 0.126-fold) and differentiated cells (1.000 ± 0.100-fold, P< 0.0001). However, no statistically significant difference was observed between the differentiated control and the *O. umbellata*-treated group (1.100 ± 0.173-fold, P =0.6120), suggesting that SREBP-1c expression was not specifically modulated by extract treatment at 100 µg/ mL.

Leptin expression was significantly elevated in differentiated adipocytes (1.079 ± 0.003-fold) relative

to undifferentiated cells (0.364 ± 0.006-fold, $P< 0.0001$). Treatment with *O. umbellata* maintained elevated leptin levels (1.102 ± 0.012-fold) compared to the undifferentiated control ($P< 0.0001$), showing a slight increase compared to the differentiated control ($P =0.0270$).

Conversely, adiponectin gene expression was robustly upregulated following *O. umbellata* treatment (17.820 ± 0.092-fold), demonstrating significantly higher transcript levels than both the differentiated control (0.741 ± 0.002-fold, $P< 0.0001$) and undifferentiated control groups (9.920 ± 0.090-fold, $P< 0.0001$). This increase in adiponectin mRNA suggests altered adipocyte metabolic function; however, functional insulin sensitivity and adiponectin protein levels were not directly measured in this study.

The combined gene-expression results indicate that *O. umbellata treatment* was associated with reduced expression of two important adipogenic and lipogenic markers, PPARγ and FAS, together with increased adiponectin expression. These molecular changes are consistent with the reductions in Oil Red O staining and intracellular triglyceride accumulation observed in the preceding experiments. PPARγ is a central regulator of adipocyte differentiation, and its reduced expression in the treated cells provides molecular support for the observed reduction in lipid accumulation. Similarly, reduced FAS expression may limit fatty acid biosynthesis and thereby contribute to the lower intracellular triglyceride content observed following treatment[42,43].

The lack of a significant difference in SREBP-1c expression between the differentiated control and treated groups suggests that the effect of *O. umbellata may* not involve substantial modulation of this transcription factor under the experimental conditions used. This observation is important because it indicates that the reduction in lipid accumulation cannot be attributed uniformly to suppression of all measured lipogenic regulators. The increase in adiponectin expression following treatment may further indicate an alteration in adipocyte metabolic function, as adiponectin is associated with lipid metabolism and insulin sensitivity. However, because insulin sensitivity and adiponectin protein levels were not directly measured, this interpretation remains preliminary. Phytochemicals such as flavonoids, triterpenes, anthraquinones, and phenolic compounds have been reported to influence pathways involved in oxidative stress, inflammation, lipid metabolism, and adipocyte differentiation. One potential pathway is AMP-activated protein kinase (AMPK), a central regulator of cellular energy and lipid metabolism that can influence acetyl-CoA carboxylase and SREBP-1c-dependent lipogenesis and promote fatty acid oxidation[44].

Inflammatory mediators, including TNF-α and IL-6, and oxidative stress have also been implicated in adipocyte differentiation and lipid accumulation[45]. Although AMPK activity, TNF-α, IL-6, and oxidative stress markers were not directly evaluated in the present study, these pathways provide possible mechanistic explanations for the observed changes in adipogenic and metabolic markers. Such mechanisms should therefore be considered hypotheses for future investigation rather than established mechanisms of action of *O. umbellata*. The present findings further show that *O. umbellata treatment* increased adiponectin expression while reducing PPARγ and FAS expression, whereas SREBP-1c and leptin expression were not significantly different from the differentiated control. Taken together with the reduction in lipid accumulation and intracellular triglyceride levels, these findings support the potential of *O. umbellata* to modulate adipogenic and lipid-storage processes in 3T3-L1 cells.

Further studies involving protein-level validation, pathway-specific assays, and functional measurements of lipid metabolism will be required to establish the molecular mechanisms responsible for these effects and to determine whether the observed cellular responses translate to anti-obesity effects *in vivo*.

Conclusion

This study demonstrates that ethanolic extracts of *Diospyros ebenum* and *Oldenlandia umbellata* possess *in vitro* inhibitory activity against key enzymes involved in carbohydrate and lipid metabolism, with *O. umbellata* showing comparatively stronger activity across the evaluated assays. At the selected non-cytotoxic concentration, *O. umbellata* reduced lipid accumulation and intracellular triglyceride levels in 3T3-L1 cells and was associated with reduced expression of PPARγ and FAS and increased adiponectin expression. These findings provide experimental evidence for the potential of *O. umbellata* to modulate adipogenic and lipid-storage processes under the conditions

investigated. GC-MS profiling together with *in silico* ADME, drug-likeness, and toxicity assessment identified several putative phytoconstituents with favorable predicted properties, providing candidates for further investigation. However, the present findings do not establish the contribution of individual compounds or the precise molecular mechanisms underlying the observed effects. Further studies involving isolation and structural confirmation of active compounds, protein- and pathway-level validation, and *in vivo* assessment are required to establish their efficacy, safety, bioavailability, and mechanism of action. Thus, *O. umbellata* may be considered a promising source of bioactive compounds with potential anti-adipogenic and metabolic activities, rather than an established therapeutic agent for obesity.

Acknowledgement

The authors thank Sathyabama Institute of Science and Technology, Chennai, for providing the laboratory facilities and institutional support to carry out this work.

Conflict of interest

All authors declare no conflict of interest.

References

1 Okunogbe A, Nugent R, Spencer G & Ralston J, Economic impacts of overweight and obesity: current and future estimates for 161 countries. *BMJ Glob Health*, 7 (2022) e009773.

2 Athesh K, Agnel Arul John N & Sridharan G, Protective effect of *Dolichos biflorus* seed extract on 3T3-L1 preadipocyte differentiation and high-fat diet-induced obesity in rats. *Evid Based Complement Alternat Med*, 1 (2023) 6251200.

3 Ariyanto EF, Wirajati F & Rahman PH, Mechanism of action of Indonesian medicinal plants in inhibiting 3T3-L1 adipocyte differentiation: a review. *J Appl Pharm Sci*, 13 (2023) 050.

4 Alatawi FS, The potential effect of green synthesis of zinc oxide nanostructures using *Cyperus rotundus* grass extracts on the genes associated with obesity in the 3T3-L1 cell line. *J Drug Deliv Sci Technol*, 87 (2023) 104792.

5 Sridhar SNC, George G & Verma A, Natural products-based pancreatic lipase inhibitors for obesity treatment. *Nat Bioactive Comp*, 1 (2019) 149.

6 Peddio S, Padiglia A, Cannea FB & others, Common bean (*Phaseolus vulgaris* L.) α-amylase inhibitors as a safe nutraceutical strategy against diabetes and obesity: an updated review. *Phytother Res*, 36 (2022) 2803.

7 Dahlén AD, Dashi G & Maslov I, Trends in antidiabetic drug discovery: FDA approved drugs, new drugs in clinical trials, and global sales. *Front Pharmacol*, 12 (2022) 807548.

8 Altay M, Acarbose is again on the stage. *World J Diabetes*, 13 (2022) 1.

9 Shahidi F & Ambigaipalan P, Phenolics and polyphenolics in foods, beverages, and spices: antioxidant activity and health effects – a review. *J Funct Foods*, 18 (2015) 820.

10 Maridass M, Ghanthikumar S & Raju G, Preliminary phytochemical analysis of *Diospyros* species. *Ethnobot Leaflets*, 12 (2008) 868.

11 Momina SS, Sana S, Parveen MD, Sirisha L & Tajuddin M, Screening of ethanolic extract of *D. ebenum* for antidiabetic and hepatoprotective effects. *Nat Volatiles Essent Oils*, 8 (2021) 3693.

12 Baravalia Y, Kaneria M, Vaghasiya Y, Parekh I & Chanda S, Antioxidant and anti-bacterial activity of *Diospyros ebenum* Roxb. leaf extracts. *Turk J Biol*, 33 (2009) 159.

13 Siva R, Status of natural dyes and dye-yielding plants in India. *Curr Sci*, 92 (2007) 916.

14 Behera BSK, Rajasekaran C, Payas S, Fulzele DP, Doss CGP & Siva R, *In vitro* flowering in *O. umbellata* L. *J Ayurveda Integr Med*, 9 (2018) 99.

15 Bhatcha MK, Review on herbal drug for TB/ethnopharmacology of tuberculosis. *Int J Pharm Res*, 1 (2013) 1.

16 Mahibalan S, Rao PC, Khan R, Basha A, Siddareddy R, Masubuti H, Fujimoto Y & Begum AS, Cytotoxic constituents of *O. umbellata* and isolation of a new symmetrical coumarin dimer. *Med Chem Res*, 25 (2016) 466.

17 Gebrehiwot H, Melaku Y, Aliye M, Ensermu U, Dekebo A, Endale M, Rentsch D & Hunsen M, Antibacterial and antioxidant efficacies of secondary metabolites from the roots of *Cyphostemma adenocaule*: a combined *in vitro* and *in silico* study. *J Trop Med*, 2024 (2024) 1679695.

18 Vijayan K, Gopinathan M & Ambikapathy V, Phytochemical screening and antioxidant activity of *Diospyros ebenum* J. Koening ex Retz leaves extract. *Int J Pharm Sci Res*, 11 (2020) 5163.

19 Vijayarathna S & Sasidharan S, Cytotoxicity of methanol extracts of *Elaeis guineensis* on MCF-7 and Vero cell lines. *Asian Pac J Trop Biomed*, 2 (2012) 826.

20 McCue PP & Shetty K, Inhibitory effects of rosmarinic acid extracts on porcine pancreatic amylase *in vitro*. *Asia Pac J Clin Nutr*, 13 (2004) 101.

21 Watanabe J, Kawabata J, Kurihara H & Niki R, Isolation and identification of α-glucosidase inhibitors from Tochu-cha (*Eucommia ulmoides*). *Biosci Biotechnol Biochem*, 61 (1997) 177.

22 Etoundi CB, Kuate D, Ngondi JL & Oben J, Anti-amylase, anti-lipase and antioxidant effects of aqueous extracts. *J Nat Prod*, 3 (2010) 165.

23 Kavitha R, Phytochemical screening and GC-MS analysis of bioactive compounds present in ethanolic extracts of leaf and fruit of *Trichosanthes dioica* Roxb. *Int J Pharm*, 12 (2020) 2755.

24 Rai M, Singh AV, Paudel N, Kanase A, Falletta E, Kerkar P, Heyda J, Barghash RF, Pratap Singh S & Soos M, Herbal concoction unveiled: a computational analysis of phytochemicals' pharmacokinetic and toxicological profiles using novel approach methodologies (NAMs). *Curr Res Toxicol*, 5 (2023) 100118.

25 Florento L, Matias R, Tuaño E, Santiago K, Dela Cruz F & Tuazon A, Comparison of cytotoxic activity of anticancer

drugs against various human tumor cell lines using *in vitro* cell-based approach. *Int J Biomed Sci*, 8 (2012) 76.

26 Balakrishnan BB, Krishnasamy K & Choi KC, Moringa concanensis Nimmo ameliorates hyperglycemia in 3T3-L1 adipocytes by upregulating PPAR-γ, C/EBP-α *via* Akt signaling pathway and STZ-induced diabetic rats. *Biomed Pharmacother*, 103 (2018) 719.

27 Bucolo G & David H, Quantitative determination of serum triglycerides by the use of enzymes. *Clin Chem*, 19 (1973) 476.

28 Livak KJ & Schmittgen TD, Analysis of relative gene expression data using real-time quantitative PCR and the 2(-Delta Delta C(T)) method. *Methods*, 25 (2001) 402.

29 Kumar VS, Kumaresan S, Tamizh MM, Islam MIH & Thirugnanasambantham K, Anticancer potential of NF-κB targeting apoptotic molecule "flavipin" isolated from endophytic *Chaetomium globosum*. *Phytomedicine*, 61 (2019) 152830.

30 Kumar P, Rani AMS, Venkatesan M, Mangammal P, Angelin JA & Subbulakshmi V, Cultivation and management of *Diospyros ebenum* (Ceylon ebony). *Vigyan Varta*, 6 (2025) 10.

31 Direito R, Rocha J, Sepodes B & Eduardo-Figueira M, From *Diospyros kaki* L. (persimmon) phytochemical profile and health impact to new product perspectives and waste valorization. *Nutrients*, 13 (2021) 3283.

32 Ahmed AH & Mahmud AF, Pharmacological activities of *Diospyros mespiliformis*: a review. *Int J Pharm Biol Sci*, 7 (2017) 93.

33 Dewanjee S, Maiti A, Kundu M & Mandal SC, Hypoglycemic activity of *Diospyros peregrina* fruits in diabetic rats. *Adv Tradit Med*, 8 (2008) 279.

34 Elwon CAM, Shah MD & Iqbal M, Hypoglycemic and hypolipidemic effects of *Oldenlandia corymbosa* against alloxan-induced diabetes mellitus in rats. *Int J Pharm Sci*, 12 (2020) 34.

35 Xie F, Wang H, Cao Q, Chen Q & Lin F, The effects of *Oldenlandia diffusa* water extract on glucose metabolism and inflammation level in rats with streptozotocin-induced gestational diabetes mellitus. *Qual Assur Saf Crops Foods*, 14 (2022) 24.

36 Han X, Guo J, You Y, Zhan J & Huang W, p-Coumaric acid prevents obesity *via* activating thermogenesis in brown adipose tissue mediated by mTORC1-RPS6. *FASEB J*, 34 (2020) 7810.

37 Omodara OO, Kawu MU, Bako IG, Mhya DH & Dawus TT, Ursolic acid attenuates obesity-related metabolic dysfunction *via* modulation of peroxisome proliferator activated receptor-gamma in male Wistar rats fed with high-carbohydrate high-fat diet. *Beni-Suef Univ J Basic Appl Sci*, 14 (2025) 2.

38 Ersoy E, Yıldızhan RB, Yılmaz MA, Yeşil Y, Şahin H, Özkan EE, Boğa M, Investigating the pharmacological potential of *Micromeria myrtifolia* Boiss. & Hohen.: phenolic profiling and biological activity assessments. *Commagene J Biol*, 8 (2024) 103.

39 Sabarathinam S, Satheesh S & Raja A, A computer-aided insight into the identification of significant therapeutic flavone as a promising agent for sarcopenic obesity. *Nat Prod Res*, 38 (2024) 2091.

40 Saraphanchotiwitthaya A & Sripalakit P, Inhibition of lipid accumulation in 3T3-L1 adipocytes by *Morinda citrifolia* Linn. leaf extracts and commercial herbal formulas for weight control. *Int J Pharm Pharm Sci*, 8 (2016) 199.

41 Chang E & Kim CY, Natural products and obesity: a focus on the regulation of mitotic clonal expansion during adipogenesis. *Molecules*, 24 (2019) 1157.

42 Jemai R, Drira R, Fetoui H, Makni M & Sakamoto K, Colocynth (*Citrullus colocynthis*) flesh extract suppresses adipogenesis by down-regulating adipogenic transcription factors and their target genes in 3T3-L1 preadipocytes. *Food Nutr Sci*, 9 (2018) 1014.

43 Hengpratom T, Ngernsoungnern A, Ngernsoungnern P, Lowe GM & Eumkeb G, Antiadipogenesis of *Oroxylum indicum* (L.) Kurz extract *via* PPARγ2 in 3T3-L1 adipocytes. *Evid Based Complement Alternat Med*, 2020 (2020) 6720205.

44 Oruganti L, Reddy Sankaran K, Dinnupati HG, Kotakadi VS & Meriga B, Anti-adipogenic and lipid-lowering activity of piperine and epigallocatechin gallate in 3T3-L1 adipocytes. *Arch Physiol Biochem*, 129 (2023) 1152.

45 Woonnoi W, Suttithumsatid W, Muneerungsee N, Saetan J, Tanasawet S & Sukketsiri W, Sangyod rice extract inhibits adipocyte growth and differentiation *via* mTOR, Akt, and AMPK pathways. *J Funct Foods*, 111 (2023) 105913.